Article

Not peer-reviewed version

Plasma and Myocardial miRNomes Similarities and Differences during Cardiac Remodelling and Reverse Remodelling in a Murine Model of Heart Failure with Preserved Ejection Fraction

Sara-Ève Thibodeau , Emylie-Ann Labbé , Élisabeth Walsh-Wilkinson , Audrey Morin-Grandmont , Marie Arsenault , Jacques Couet *

Posted Date: 27 June 2024

doi: 10.20944/preprints202406.1909.v1

Keywords: mouse; heart failure; myocardial recovery; reverses remodelling; cardiac hypertrophy; microRNA; preclinical model

Article

Plasma and Myocardial miRNomes Similarities and Differences during Cardiac Remodelling and Reverse Remodelling in a Murine Model of Heart Failure with Preserved Ejection Fraction

Sara-Ève Thibodeau [1,2], Emylie-Ann Labbé [1,2], Élisabeth Walsh-Wilkinson [1], Audrey Morin-Grandmont [1], Marie Arsenault [1] and Jacques Couet [1,*]

[1] Groupe de recherche sur les valvulopathies, Institut Universitaire de Cardiologie et de Pneumologie de Québec - Université Laval, Quebec, Canada
[2] These authors contributed equally to this work.
* Correspondence: jacques.couet@med.ulaval.ca

Abstract: Heart failure with preserved ejection fraction (HFpEF) is a heterogeneous syndrome characterized by multiple risk factors and associated conditions. HFpEF prevalence is rising, and its prognosis remains poor after the first hospitalization. Using a two-hit HFpEF murine model, we aimed at studying cardiac reverse remodelling after stopping the causing stress (Angiotensin II [AngII]) and a high-fat diet [HFD]; MHS) and introducing voluntary exercise. We studied in young male and female C57Bl6/J mice fed or not with an HFD (60% calories from fat) the cardiac response to AngII (1.5 mg/kg/day for 28 days). Then, MHS was stopped, and VE was started for another four weeks (RR). We studied the effects of MHS and RR on the circulatory microRNA (miR) profile (miRNome) and the myocardial miRNome to characterize the cardiac and non-cardiac response of small RNAs. AngII alone and MHS but not the HFD caused cardiac hypertrophy (CH), left ventricular (LV) concentric remodelling and left atrial enlargement in male mice. HFD-induced CH and LV concentric remodelling only in female mice. Four weeks after RR, CH, LV concentric remodelling and atrial enlargement were reversed. We performed bulk circulatory and LV miR sequencing. We did not observe differences linked to biological sex. RR restored normality for circulatory miRNome, whereas LV miRNome remained relatively similar to the one after MHS. Among the 25 most abundant circulatory miRs, ten were modulated by MHS (9 upregulated). In the LV, 8 of the 25 most abundant miR were upregulated by MHS, and 10 were downregulated. MiRNomes from AngII, HFD or MHS shared many common modulated miRs (32), suggesting that the overall response of organs producing the bulk of circulatory small non-coding RNA was similar even for seemingly different stress.

Keywords: mouse; heart failure; myocardial recovery; reverse remodelling; cardiac hypertrophy; microRNA; preclinical model

1. Introduction

Heart failure (HF) is divided into three basic categories based on left ventricular (LV) ejection fraction (EF): HF with preserved ejection fraction (HFpEF; EF ≥ 50%), HF with reduced EF (HFrEF; EF < 40%), and HF with midrange EF (HFmEF, EF ≥ 40 and < 50%) [1]. Patients with HFpEF are often older, more of them female, hypertensive and obese [2]. Patients with HFpEF have higher rates of morbidities, mortality, and rehospitalization than those with HFrEF and have poorer quality of life [3].

HFpEF is a multifactorial disease displaying various phenotypes. Age, hypertension, and female sex are classical risk factors contributing to its development. Atrial fibrillation is also present in a significant portion of patients suffering from HFpEF. A cardiometabolic phenotype, including obesity and type 2 diabetes mellitus, has become more prevalent in recent years [4,5].

The development of efficient medical therapies for HFpEF has lagged behind the one made for HFrEF, where many drugs have been proven helpful in reducing the burden of symptoms and

 doi:10.20944/preprints202406.1909.v1

improving survival [6]. The recent EMPEROR-Preserved clinical trial has yielded encouraging results, showing for the first time that a medication (SGLT2 inhibitors) could benefit significant clinical endpoints in HFpEF [7]. This has come after years of unsuccessful trials with many classes of drugs that sometimes had shown clear benefits in HFrEF.

Aerobic exercise training has emerged as one of the most effective means of improving outcomes in patients with HFpEF. Therapeutic strategies for managing this population should probably combine a pharmacological intervention with one targeting lifestyle changes. Multiple randomized clinical trials of supervised exercise training in selected patients with chronic and stable HFpEF showed that exercise could provide clinically relevant improvements in exercise capacity and quality of life. Lifestyle changes constantly show improvement in studies conducted in HFpEF patients [8].

The search for specific biomarkers has been an ever-expanding research effort to assess the efficacy of these interventions [9]. Among potential circulatory biomarkers, microRNAs (miRs) have emerged as exciting targets and possible therapeutic agents for HF [10]. MiRs are small (22 nucleotides) non-coding RNA able to repress messenger RNA translation or cause its degradation [11]. The underlying dysregulation of the cardiac transcriptome or the miRNome in myocardial remodelling, reverse remodelling (RR), or HF has been studied in the past [12–17]. Several studies have described the expression of different sets of miRs in the myocardium and circulation of human HF patients [18–21]. Comparing those two miRNomes after myocardial remodelling and RR has received less attention, especially in HFpEF.

The availability of suitable HFpEF animal models reflecting different phenotypes has progressed significantly in recent years. In the mouse, HFpEF models triggered by a single factor (hypertension, obesity/diabetes or aging) have been replaced by more complex models combining more than one factor [22].

Here, we use a “two-hit” murine HFpEF (Angiotensin II (AngII) + High-Fat Diet (HFD); MHS) to study whether stopping AngII, normalizing the diet, and introducing voluntary exercise (VE) could help reverse cardiac damage and improve exercise intolerance. In addition, we aimed to describe better the circulatory and myocardial miRNome's response to stress and to characterize its eventual normalization afterwards [23]. Our main aim was to identify miR markers of myocardial reverse remodelling.

We show that MHS for 28 days in 8-week-old male and female mice induced a light HFpEF phenotype combining cardiac hypertrophy (CH), concentric LV remodelling, left atrial enlargement and reduced exercise capacity. After stopping MHS, four additional weeks normalized CH, concentric LV remodelling and increased exercise capacity. We observed extensive changes in the circulatory and myocardial miRNomes after MHS. Only the circulatory miRNome was normalized after RR, whereas the myocardial miRNome remained abnormal.

2. Materials and Methods

2.1. Animals

C57BL6/J male and female 7-week mice were purchased from Jackson Laboratory (Bar Harbor, ME, USA). Mice were housed on a 12h light-12 h dark cycle with free access to chow and water. The protocol was approved by the Université Laval's animal protection committee and followed the recommendations of the Canadian Council on Laboratory Animal Care (#2020-603 and #2023-1250).

2.2. Experimental design

Mice were randomly distributed in the various experimental groups. We used a two-hit HFpEF model we recently described [22]. A. 48 two-month-old mice were divided into four groups (n=6) as male (M) or female (F) implanted or not with an osmotic minipump providing a continuous infusion of angiotensin II (AngII; 1.5mg/kg/day) (Sigma) for 28 days and fed or not with a high-fat diet (HFD: 60% calories from fat, 20% from protein and 20% from carbohydrates; Research Diets Cat. #D12492). The standard diet had 10% calories from fat (D12450J). These mice were followed by echocardiography (echo) at baseline (8-week-old) and the day before euthanasia. B. A second batch

 doi:10.20944/preprints202406.1909.v1

of mice received AngII + HFD (MHS) for four weeks. Then, on day 28, osmotic minipumps were removed, and the diet of HFD-fed mice was changed to the standard diet (RR). The same day, a flying saucer-type exercise device was introduced in their cage (Innowheel™, Innovive, Billerica, MA, USA). Twenty-eight days later, the protocol was stopped. Mice had an echo exam on day 55 and were euthanatized the day after. The heart was weighted and harvested. The animal's behaviour was monitored daily by experienced Technicians for health and behaviour during the protocol. The animals were weighed weekly. No mouse displayed signs associated with poor prognosis of quality of life or specific signs of severe suffering or distress. Among those signs, significant loss or gain of weight, grooming and changes in behaviour were recorded.

2.3. Echocardiography

Echocardiography, osmotic mini-pump surgery, and euthanasia were performed under isoflurane anesthesia as described previously [24,25]. The same investigator, blinded for mouse identification, acquired Echo images on a Vevo 3100 imaging system (VisualSonics, FujiFilm, Toronto, Canada). Transthoracic echocardiography was performed using a 40 MHz image transducer (MX550S).

2.4. RNA Isolation

Total RNA from LV tissue was extracted using TRI Reagent (Sigma), as described previously (22). Plasma (200µl) total RNA, including miRNA, was extracted using the Qiagen miRNeasy Serum/Plasma Advanced Kit following suppliers' instructions (Qiagen, Inc, Toronto, ON).

2.5. RNA Preparation for Sequencing

Immediately after total RNA extraction, DNAse treatment of LV sample, long RNA (>200 bp, mRNA), and small RNA (<200 bp) were separated using different ethanol percentage solutions and Qiagen mini-Kit columns. When necessary, samples were cleaned using the Qiagen RNeasy MinElute Cleanup Kit to remove genomic DNA traces. RNA integrity and quality (RIN averaging 8.8 (8.1-9.1)) were acquired using Agilent Technologies 2100 Bioanalyzer, namely using an RNA-specific chip (Agilent Eukaryote Total RNA Nano 1000). To measure complementary DNA (cDNA) library concentrations, the Kapa Universal Library Quantitation kit was used (Roche).

2.6. Bulk microRNA-Sequencing

RNA samples were processed with the Qiagen miRNA Library kit following the manufacturer's recommendations. Each sample was constituted of RNA from one mouse, either male or female. Sequencing libraries were analyzed using an Agilent Bioanalyzer to verify their size. An aliquot of the library was run on a 6% PAGE gel, and a band at 175 bp corresponding to the expected size of the library was excised and purified. Indexed libraries were pooled and sequenced on the Illumina NextSeq 2000 (single-end 75 bp) according to the manufacturer's protocols. An average number of 6.8 million reads per sample was obtained. Micro RNA-Seq Alignment was processed on the Qiagen RNA portal for sequence alignment using the Mus musculus miRBase version 22 (GRCm38.101) reference genome. Around 80% of UMI reads were annotated with the miRBase for left ventricle samples and 15% for plasma samples. The differentially regulated microRNAs were identified with a false discovery rate (FDR) ≤ 0.05, a Log2 fold change (Log2FC), |Log2 FC| ≥ 1 and a normalized count exceeding 10. Volcano plots and heat maps were then generated using this Qiagen platform.

2.7. MicroRNA analyses

The miRNEt (www.mirnet.ca) tools were used to determine potential miRNA-target interactions and built network-based analysis. For the modulated plasma miRs, we used the TargetScan database to determine possible targets. For the myocardial miRs, we created a functional network by pairing upregulated miRs with differentially regulated LV genes after MHS from a Previous study [22]. The

 doi:10.20944/preprints202406.1909.v1

same was done for downregulated miRs [26,27]. Cytoscape software was used to build the illustration [28].

2.8. Plasma Inflammatory Marker Measurements

The mouse plasma inflammatory protein content was externally characterized by Olink Proteomics® (Uppsala, Sweden) using a proteomics assay simultaneously measuring 43 proteins per sample (Olink Target 48 Mouse Cytokine Panel). In brief, this assay involves protein-specific antibody pairs labelled with unique complementary oligonucleotides (probes) being added to 1 µL of sample in a 96-well plate. Only when both antibodies in the pair bind to the corresponding protein are their attached probes close enough to hybridize. This generates a polymerase chain reaction (PCR) target sequence amplified and detected using a standard real-time PCR protocol. Thirty cytokines of 43 passed the level of quantification and could be measured in the plasma of the animals. Four animals for each of these groups were evaluated: male or female and control or MHS.

2.9. Statistical Analysis

All data are expressed as mean ± standard error of the mean (SEM). Intergroup comparisons were conducted using students' T-tests using GraphPad Prism 10 (GraphPad Software Inc., La Jolla, CA, USA). Comparisons of more than two groups were analyzed using one-way or two-way ANOVA and Holm-Sidak post-test. $P<0.05$ was considered statistically significant.

3. Results

3.1. Angiotensin II alone or Combined with a High-Fat Diet Induces Cardiac Hypertrophy in Male and Female Mice

Male and female mice (n=6/group) were administered AngII alone or in combination with a high-fat diet for 28 days. In males, AngII reduced body weight, whereas in females, HFD did the opposite (Figure 1A-B). When combined (MHS), body weight remained unchanged.

After 28 days, AngII alone or combined with the HFD (MHS) significantly increased both males' and females' heart and left atrial weights. HFD only caused cardiac hypertrophy and left atrial enlargement in females (Figure 1B). Lung congestion was evaluated by weighing lungs at the time of euthanasia. Only in females fed with the HFD did we observe an increase in lung weight.

An echo exam was performed the day before euthanasia. Combined interventricular septal wall and posterior wall thickness (LV walls) were increased by AngII, HFD and MHS in males and only by AngII and MHS in females (Figure 1C-D). End-diastolic LV diameter (EDD) remained unchanged in males but was reduced by MHS in females. This resulted in an increased relative LV wall thickness ratio (RWT) in both AngII or MHS males and females. Ejection fraction (EF) was unchanged for all groups. Additional echo data are included in the supplementary Tables S1 and S2.

 doi:10.20944/preprints202406.1909.v1

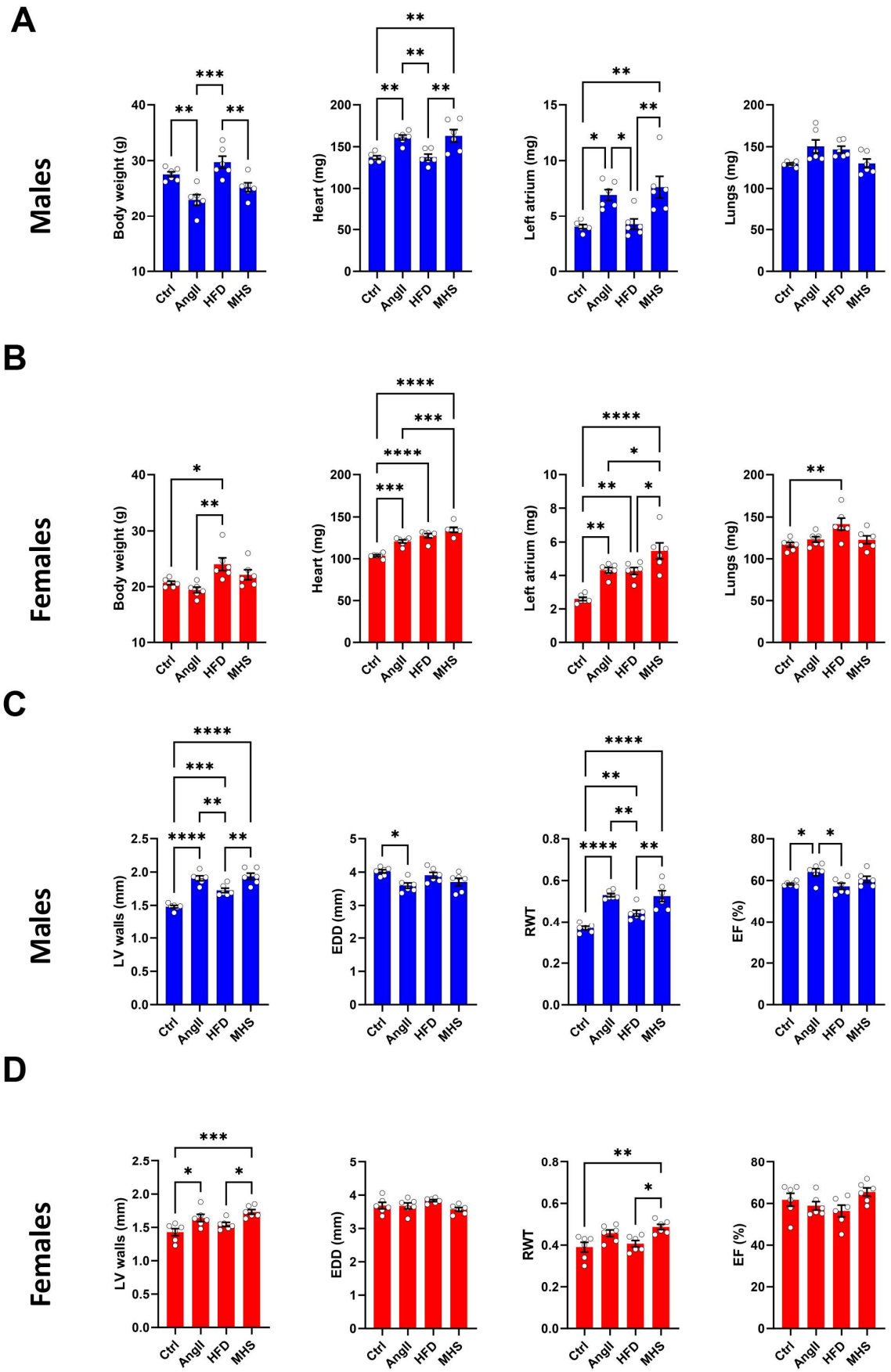

 doi:10.20944/preprints202406.1909.v1

Figure 1. AngII alone or combined (MHS) with HFD induces cardiac hypertrophy and left atrial enlargement in male and female mice. A. Males. Data at euthanasia (n=6/group). AngII and MHS increased heart and left atrial weight but not lung weight. B. Females. HFD causes obesity, cardiac hypertrophy, left atrial enlargement and lung congestion. AngII and MHS increased heart and left atrial weight. C. Males. Echo data. AngII and/or HFD increased LV wall thickness and relative wall thickness (RWT) without reducing ejection fraction (EF). D. Females. MHS had the strongest effects on LV wall thickening and RWT. Data are represented as mean +SEM. One-way ANOVA followed by Holm-Sidak post-test. *: $p<0.05$, **: $p<0.01$, ***: $p<0.001$ and ****: $p<0.0001$ between indicated groups.

3.2. Circulatory miRNomes of Mice Receiving Either AngII or HFD or a Combination of Both (MHS) Show Many Common Modulated microRNAs

We performed bulk microRNA sequencing on plasma fractions of AngII, HFD and MHS mice to assess their effects on the circulatory miRNome. We did not observe apparent sex-specific Differences in control mice circulatory miRNomes, so the results presented afterwards combined data from both male and female mice. As illustrated in Figure 2A in Venn diagrams, dysregulated miRs (Fold change $>|\log_2 1|$ and false discovery rate [FDR] <0.05) compared to control animals of AngII, HFD or MHS mice show that a good proportion of these are common even for stresses as different as AngII and HFD. Similarities were also present for the profile of upregulated and downregulated miRs (Figure 2B-D) between AngII mice and HFD mice.

 doi:10.20944/preprints202406.1909.v1

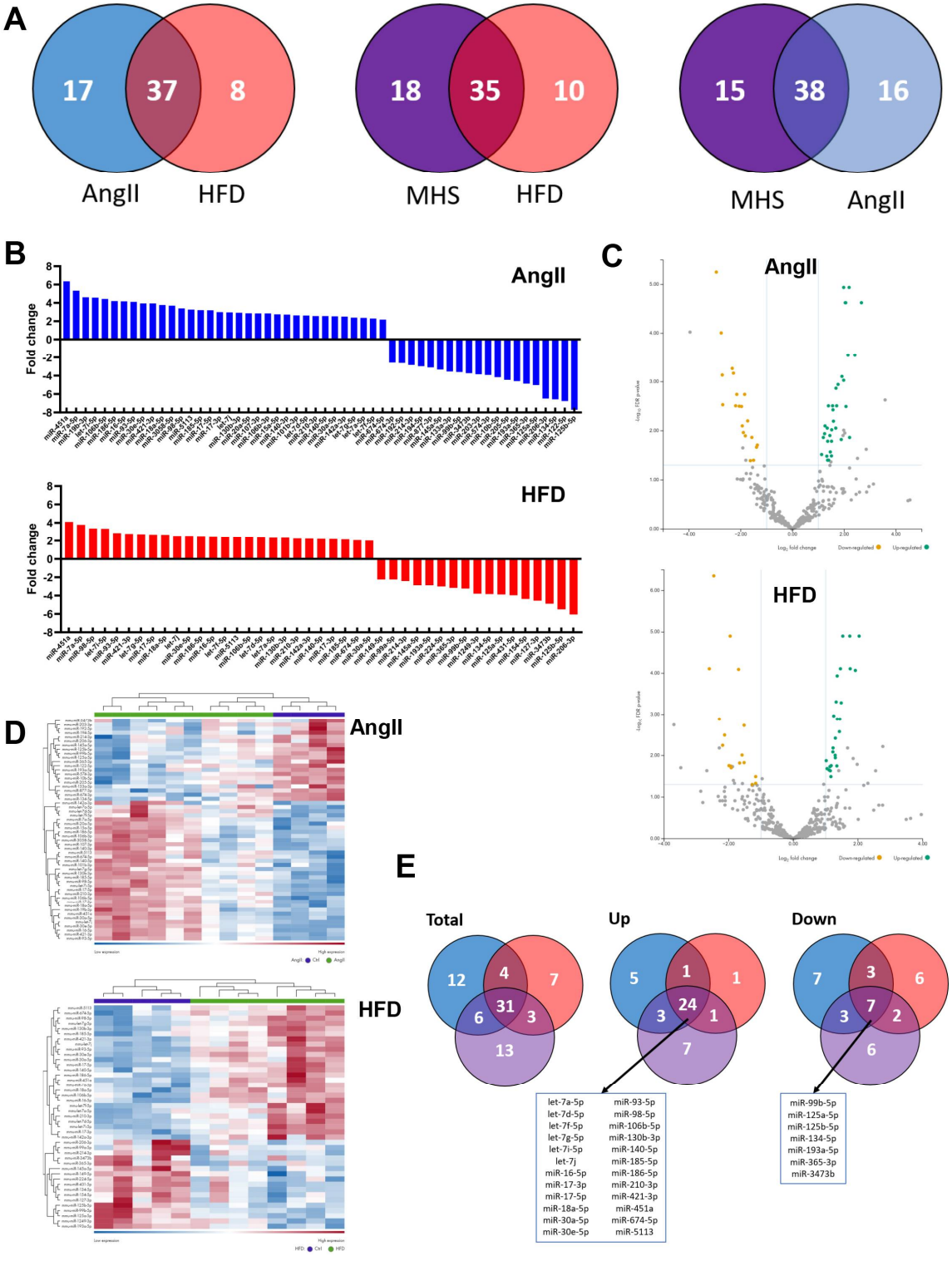

Figure 2. Alteration of the plasma miRNomes after four weeks of AngII, HFD or MHS. A. Venn diagrams illustrating the number of modulated miRs between the control group and the indicated stress group. (AngII: blue, HFD: red or MHS: purple). Many modulated miRs between each stress group were common. B. Upregulated and downregulated circulating miR after four weeks of AngII (blue) or HFD (red). Graphs represent fold change (log_2) of all significantly modulated miRs (FDR<0.05) after four weeks of the indicated stress. C) Volcano plots of differently expressed miRs after AngII (up) or HFD (bottom). Green dots illustrate upregulated miRs, and yellow dots downregulated ones. Grey dots either had a fold change below ±2 or had a false discovery rate (FDR) over 0.5. D) Heat maps of modulated miRs after AngII (up) and HFD (bottom) stress compared to

 doi:10.20944/preprints202406.1909.v1

control mice. Purple samples are controls, and green ones are AngII or HFD. Colours range from blue (low expression) to red (high expression). E) Venn diagrams of modulated miRs in AngII (blue), HFD (red) and MHS (purple) compared to control animals. Thirty-one miRs are shared between the three stresses. Twenty-four are upregulated, and seven are downregulated. These miRs are listed below the Venn diagrams.

A set of 31 miRs were dysregulated by AngII, HFD and MHS (listed in Figure 2E); 24 were upregulated, and seven were downregulated. Using miRNet 2.0 and the TargetScan database, we identified target genes for the 24 upregulated miRs [26,27,29,30].

Figure 3A illustrates a network of 1200 possible mRNA targets for the 24 upregulated miRs. We differentiated between the highly, the mid and the lowly expressed miRs in the network. Among the highly expressed circulatory miRs, mir-30-5p and mir-30a-5p had the most potential mRNA targets, with 382 and 51, respectively. As illustrated in Figure 3B, an enrichment for genes encoding transcription factors was observed among the miR targets. Interestingly, three signalling pathways were identified from the KEGG database, as illustrated in Figure 3C, namely Pi3K-Akt, MAP kinase and JAK-STAT pathways, all known for their implication in cardiac hypertrophy (REF). The Th17 cells differentiation pathway was also enriched.

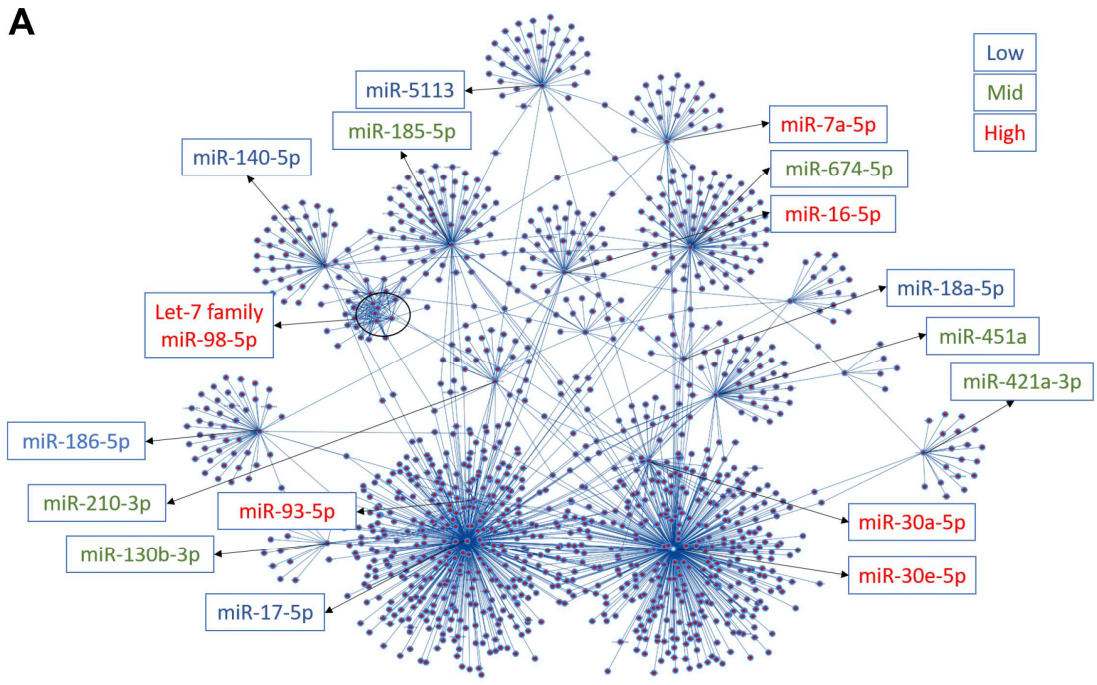

B

GO Molecular function	FDR
protein binding	2.65E-30
enzyme binding	1.19E-12
transcription factor binding	1.16E-07
DNA-binding transcription factor binding	3.52E-07
binding	1.57E-06
chromatin binding	3.67E-06
ion binding	4.93E-06
catalytic activity, acting on a protein	6.66E-06
RNA polymerase II-specific DNA-binding TF binding	1.53E-05
protein domain specific binding	1.90E-05

C

KEGG	FDR
Pathways in cancer	5.53E-11
Inflammatory bowel disease	3.40E-07
Colorectal cancer	8.33E-07
Cellular senescence	2.28E-06
PI3K-Akt signaling pathway	2.60E-06
MAPK signaling pathway	3.72E-06
JAK-STAT signaling pathway	3.49E-05
Th17 cell differentiation	3.95E-05
Prostate cancer	4.10E-05
Hepatitis B	6.18E-05

Figure 3. A. Interactome network of the 24 common plasma miRs with their potential target from the TargetScan database. This network was generated using the miRNet 2.0 analytical tool and Cytoscape to build the illustrated network. The location of the plasma miRs is indicated and was classed in tertiles (low, blue, mid, green, high, and red) based on their normalized counts after sequencing. Dots

 doi:10.20944/preprints202406.1909.v1

represent target genes. B. Go molecular functions ten most significant categories from the interactome (FDR: false discovery rate value). C. Ten most significant pathways from the KEGG database.

To explore further if pathways related to immunity and inflammation were activated in our mice, we measured a panel of 30 interleukins, cytokines, chemokines, and other related factors in the plasma of control and MHC mice. MHS modulated nine out of thirty of these factors in mice; for most factors, the variations were only present in female mice (Figure 4).

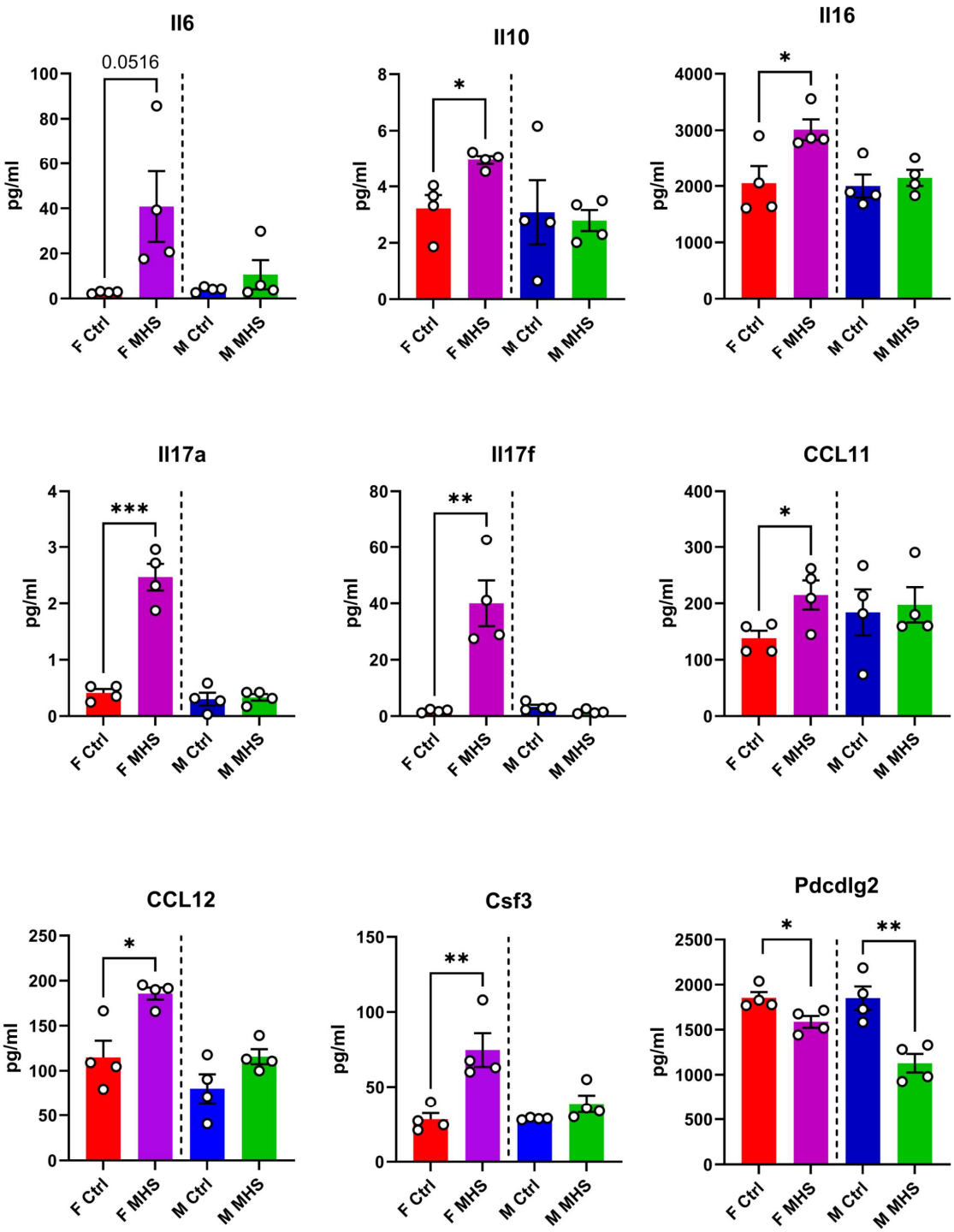

Figure 4. Plasma protein concentration of 9 immunity-related molecules in male and female mice exposed or not to MHS. Levels of these molecules were evaluated as described in the Material and

 doi:10.20944/preprints202406.1909.v1

Methods section. Il6: interleukin-6, IL10: interleukin-10, IL16: interleukin 16, IL17: interleukin 17, CCL11: C-C Motif Chemokine Ligand 11, CCL12: C-C Motif Chemokine Ligand 12, Csf3: Colony Stimulating Factor 3, and Pdcd1lg2: Programmed Cell Death 1 Ligand 2. Data are represented as mean +SEM (n=4). F: females, and M: males. Student T-test between controls (Ctrl) and MHS. *: $p<0.05$, **: $p<0.01$ and, ***: $p<0.001$ between indicated groups.

3.3. MHS Cardiac Hypertrophy Is Reversed after RR

As described above, half the MHS mice had their osmotic mini pump removed after 28 days, were fed a standard diet, and were allowed to exercise voluntarily (VE) for an additional 28 days. Cardiac hypertrophy present after MHS for 28 days was normalized at day 56 (RR; Figure 5A-B). Left atrial (LA) weight, which increased in MHS groups, was reduced after RR.

Echo data confirmed this reverse remodelling after MHS cessation and the introduction of VE, as illustrated in Figure 5C-D. LV wall thickness (IVS + PW) increased after MHS returned to control values after RR. End-diastolic diameter was like age-matched controls, and RWT increased after MHS also returned to control values. However, the ejection fraction in RR males was below those of controls.

 doi:10.20944/preprints202406.1909.v1

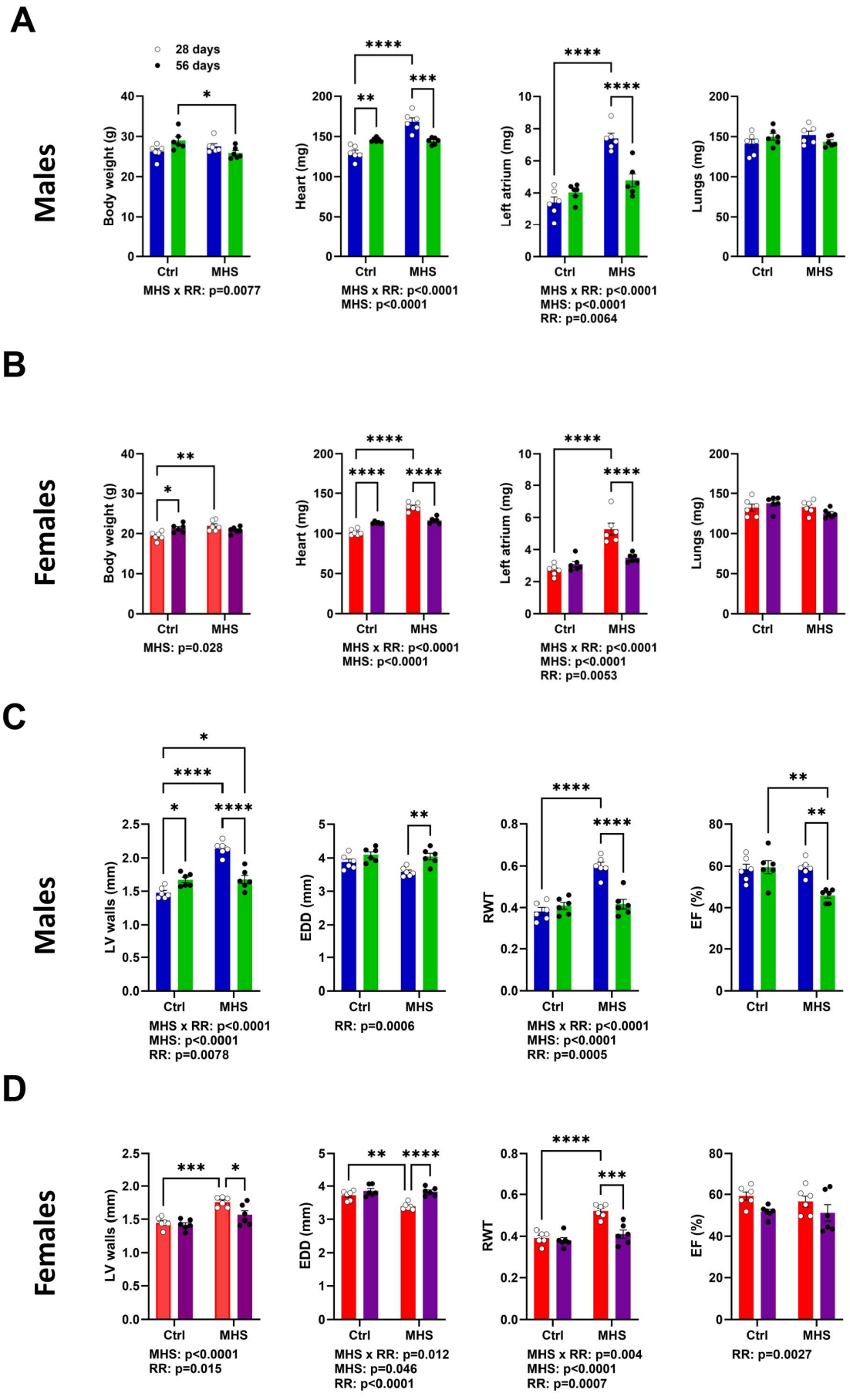

 doi:10.20944/preprints202406.1909.v1

Figure 5. Four weeks after AngII and HFD cessation and introduction of voluntary exercise reversed cardiac hypertrophy and left atrial enlargement in male and female mice. A. Males. Data at euthanasia (n=6/group) Blue columns and open dots (28 days) and green columns and black dots (56 days). MHS increased heart and left atrial weight, and RR returned these parameters to values comparable to those of age-matched control mice. B. Females. Red columns and open dots (28 days) and purple columns and black dots (56 days). MHS increased heart and left atrial weight, and RR returned these parameters to values comparable to those of age-matched control mice. C. Males. Echo data. RR returned MHS-increased LV wall thickness to normal. This was true for the end-diastolic LV diameter (EDD) and relative wall thickness (RWT) but reduced ejection fraction (EF). D. Females. RR returned MHS-increased LV wall thickness to normal. This was true for the end-diastolic LV diameter (EDD), and relative wall thickness (RWT) and ejection fraction (EF) were preserved. Data are represented as mean +SEM. Two-way ANOVA followed by Holm-Sidak post-test. *: $p<0.05$, **: $p<0.01$, ***: $p<0.001$ and ****: $p<0.0001$ between indicated groups. Factors (MHS, RR of their interaction) below $p<0.05$ are indicated below graphs.

3.4. Circulatory miRNome, But Not LV miRNome, Is Normalized after RR

More LV miRs were downregulated than upregulated after MHS compared to controls (83 vs. 73; Figure 6A). RR did not bring normalization of the myocardial miRNome, where 148 miRs were still dysregulated compared to controls (Figure 6B). Only 31 miRs differed when the MHS and the RR group were compared directly (Figure 6C). One hundred thirty-five dysregulated miRs were shared between MHS and RR mice when both groups were compared to controls (Figure 6D). A small portion of these miRs were less dysregulated in RR animals, and none had their expression normalized (Figure 6E). We then identified common miRs modulated in MHS and RR mice but in the opposite direction. Of these 20 miRs, 14 had their levels modulated toward normal levels (Figure 6F).

 doi:10.20944/preprints202406.1909.v1

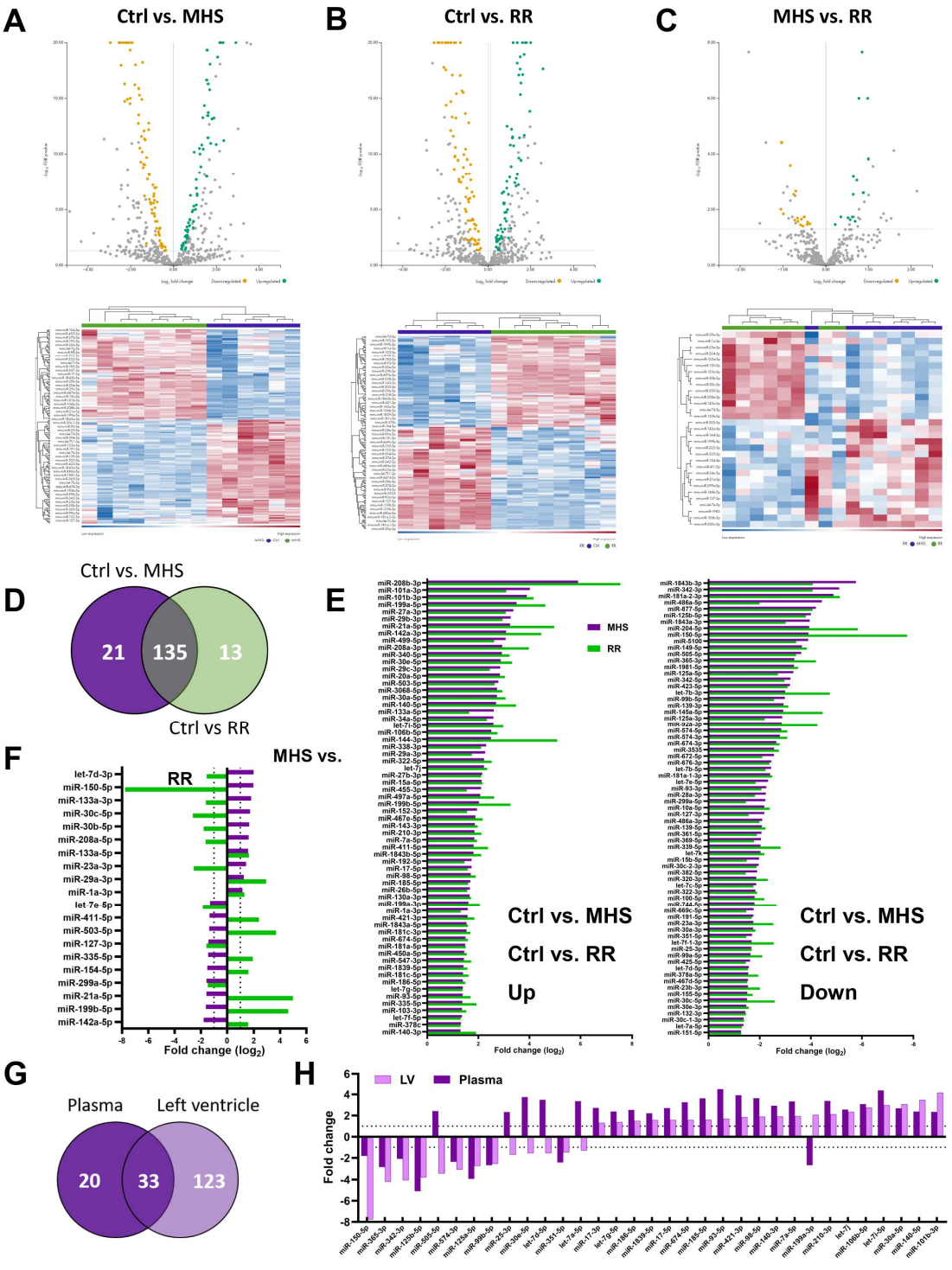

Figure 6. Alteration of the LV miRNome after four weeks of MHS and then RR. Volcano plots and heat map of differently expressed miRs after MHS compared to controls (A), RR compared to controls (B) and C, between MHS and RR. Green dots illustrate upregulated miRs and yellow dots downregulated ones. Grey dots either had a fold change below ±2 or had a false discovery rate (FDR) over 0.5. Dark blue samples are controls (MHS in C), and green ones are MHS (A) or RR (B and C). Colours range from blue (low expression) to red (high expression). D. Venn's diagram illustrates the number of modulated miRs between the control group and MHS and between the control and RR groups. (MHS: purple and RR: Green). E. All miRs upregulated (left) and downregulated (right) between control and MHS (purple) or RR (green) in the LV are modulated in the same fashion. F. Only 20 miRs are differentially modulated when comparing the LV miRNomes of the MHS group

 doi:10.20944/preprints202406.1909.v1

(purple) at 28 days and the RR group (green) at 56 days, and 12 of them are regulated in different directions. G. Most plasma miRs modulated in the LV are also modulated in the plasma. In the LV, this represents only 21% of modulated miRs. H. Most of the 33 common miRs between the plasma and LV miRNome of MHS-treated mice are modulated in the same direction (27 of 33).

We then compare the plasma and myocardial miRNome profiles in MHS mice. Almost two-thirds (33/54) of circulatory miRs dysregulated by MHS were modulated in the left ventricle, representing 13% of miRs dysregulated in the LV (Figure 6G). Levels of six of these 33 miRs were modulated differently between the plasma and the LV (Figure 6H).

Unlike the LV miRNome, four weeks of RR was sufficient to completely normalize the circulatory miRNome after MHS (Figure 7A-C). No miRs were found to be differentially expressed in the plasma between controls and RR mice (not shown).

 doi:10.20944/preprints202406.1909.v1

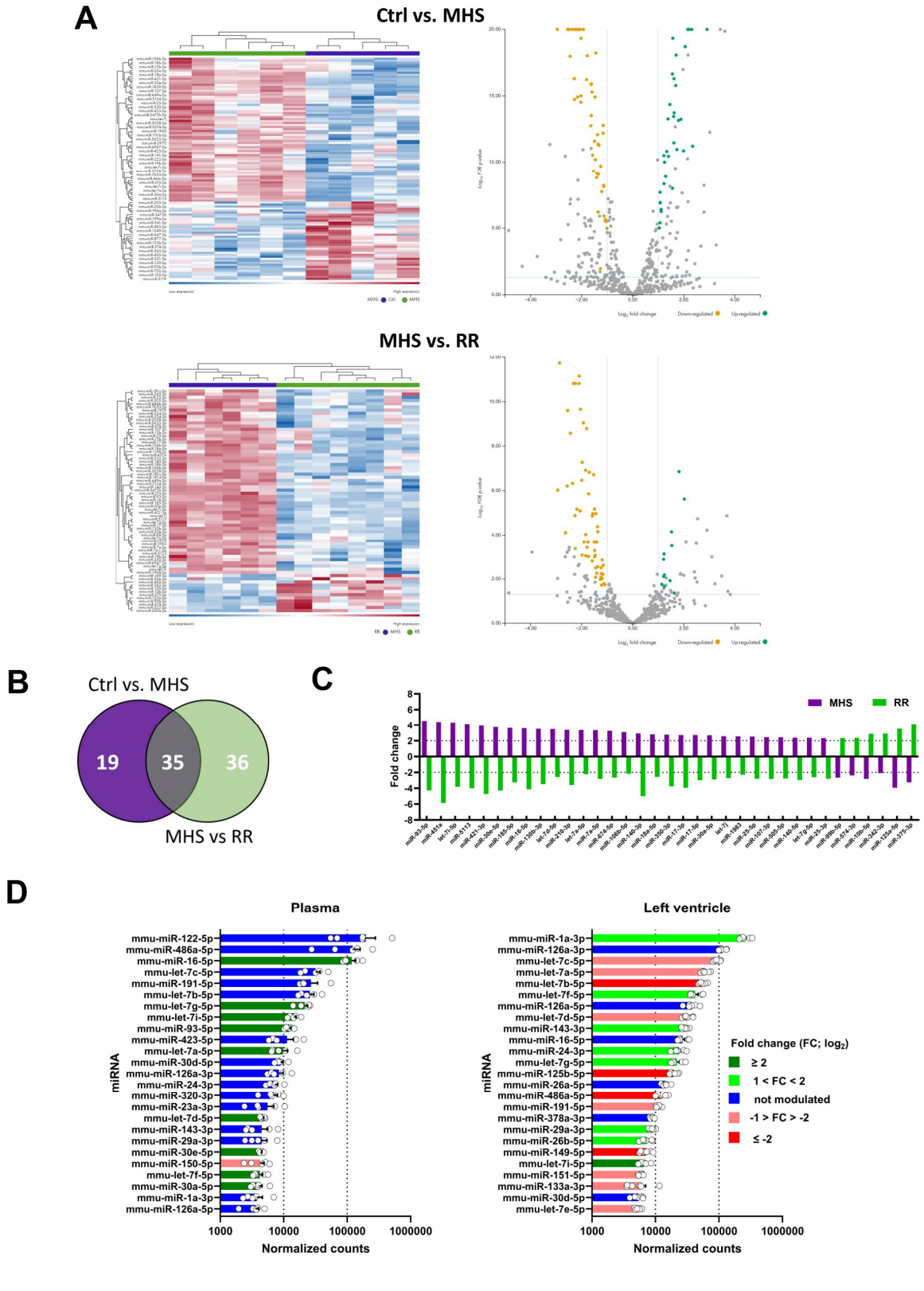

Figure 7. The circulatory miRNome is completely normalized after RR. A. Heat maps and volcano plots of differently expressed miRs after MHS (up) and RR (bottom). Green dots illustrate upregulated miRs, and yellow dots downregulated ones. Grey dots either had a fold change below ±2 or had a false discovery rate (FDR) over 0.5. B. Venn diagram illustrating the number of modulated miRs between the control group and MHS and between MHS and RR groups. (MHS: purple and RR: Green). C. All miRs upregulated or downregulated between control and MHS (purple) are modulated

 doi:10.20944/preprints202406.1909.v1

in the opposite direction in the RR (green) group. F. Changes in the most abundant miRs in the plasma and the LV after MHS. The list of the 25 most abundant miRs was established as the average normalized counts of the control samples from the plasma or the left ventricle. Light and dark green are the miRs upregulated after MHS, and those downregulated in pink and red. In blue, miRs where levels remained stable.

Using the normalized counts from the miR sequencing, we produced a list of the 25 most abundant miRs in the plasma and left ventricle. Seventeen of the 25 most abundant miRs in the plasma and the LV were identical. We determined their modulation, and only ten out of 25 were modulated in the plasma, all upregulated except for one. For the left ventricle, 19 of the most abundant miRs were modulated, 8 upregulated, and 11 downregulated. Five of these were very strongly modulated (Figure 7D).

We then crossed the dysregulated miR profile obtained from the LV with a myocardial transcriptome from MHS mice [22]. We produced a network of miRs targeting differentially expressed genes (DEGs) in the left ventricle of MHS mice. Figures 8A and 8B illustrate networks for upregulated and downregulated miRs, respectively. Among the myocardial upregulated miRs, miR-21a-50, miR-29b-3p, miR-27a-3p, miR-27b-3p, miR-15a-50 and miR-101a-5p had the most mRNA targets. Fibronectin (Fn1), transferrin receptor (Tfrc), Cyclin-Dependent Kinase Inhibitor 1A (Cdkn1a), Iodothyronine Deiodinase 2 (Dio2) and Ectonucleotide Pyrophosphatase/ Phosphodiesterase 1 (Enpp1) were the genes most targeted by miRs. Among the downregulated myocardial miRs, mir-122-5p and mir-125-5p had the most mRNA targets, with 84 and 32, respectively. Fn1 and Tfrc were among the potentially most targeted genes by the downregulated miRs. Centromere Protein F (Cenpf), NADPH Oxidase 4 (Nox4) and Solute Carrier Family 1 Member 2 (Slc1a2) followed in this order.

 doi:10.20944/preprints202406.1909.v1

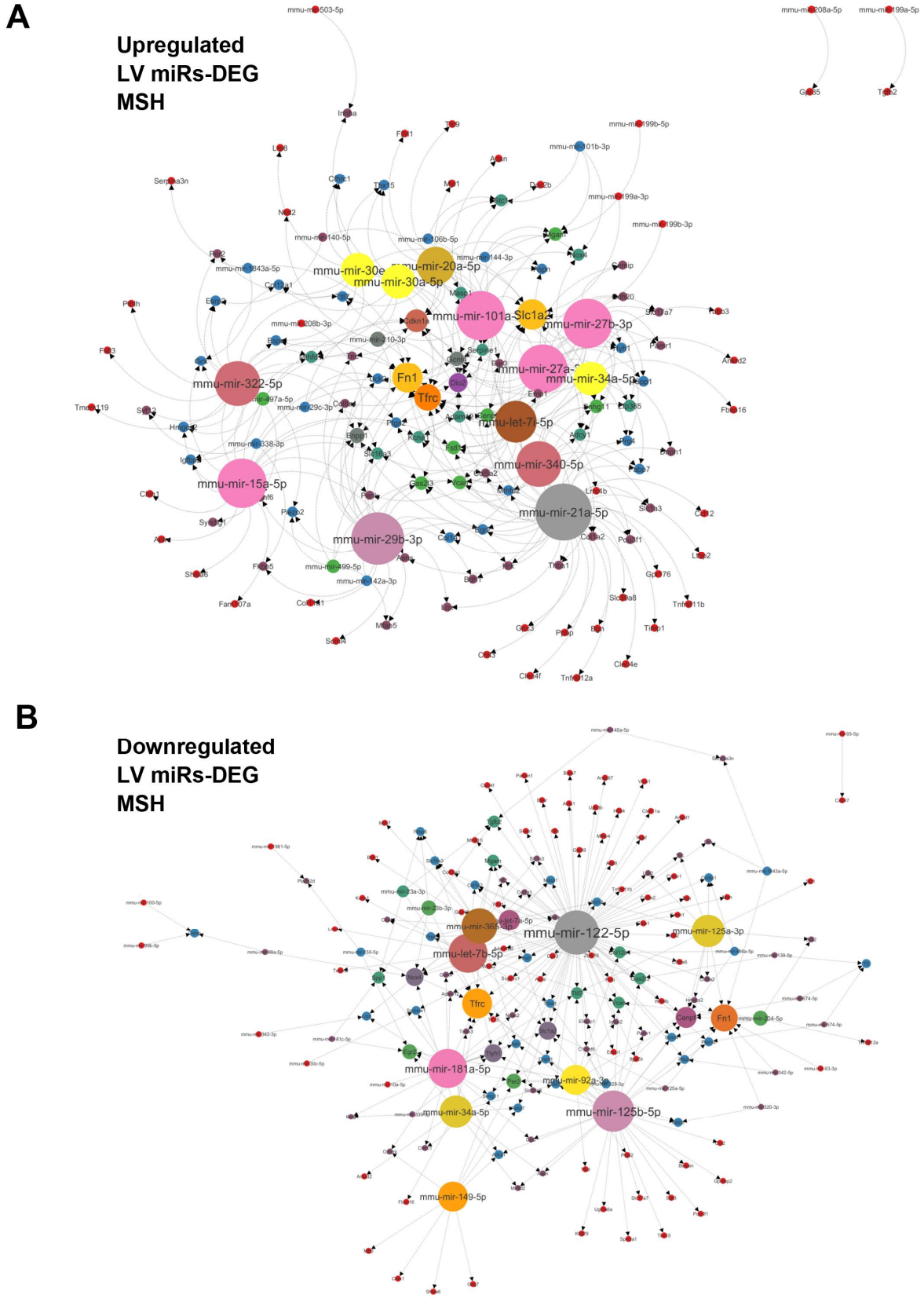

Figure 8. A. Interactome network of 34 strongly upregulated (+$\log_2$2 FC) LV miRs vs. differentially regulated genes determined after a bulk RNA sequencing of the same LV RNA samples used for determining the miRNome of MHS LV compared to controls. This network was generated using the miRNet 2.0 analytical tool and Cytoscape to build the illustration. The number of possible interactions of miRs and genes determines the sizes of each dot on the network. B. Interactome network of 49

 doi:10.20944/preprints202406.1909.v1

strongly downregulated (-log2 FC) LV miRs vs. LV differentially regulated genes after MHS compared to controls.

4. Discussion

This study used a two-hit mouse model of HFpEF combining AngII and an HFD for 28 days (MHS) [22]. This model shows many similarities with clinical HFpEF, including hypertension, obesity, preserved EF, concentric LV remodelling, left atrial hypertrophy, and reduced exercise tolerance. We observed that many of these abnormalities were reversed after stopping MHS and introducing voluntary exercise for an additional 28 days (RR). Although extensive RR was observed, myocardial recovery was still incomplete. For instance, though significantly increased from voluntary exercise in all animals, exercise tolerance stayed inferior in the RR group compared to controls. Moreover, we now show that the myocardial miRNome of RR animals did not differ much from that of MHS animals four weeks before.

Our mouse model of heart failure has some strengths and weaknesses. Unlike humans, the mice in this study were young, and their heart growth was incomplete [24]. In mice, the heart continues to gain mass throughout their lives. Female mice were not ovariectomized to simulate menopause, allowing for potential protection from ovarian hormones.

Angiotensin II infusion counterbalanced high-fat diet-induced obesity. Angiotensin II has been shown to induce lipolysis in mice, which opposes the HFD effects [31]. Therefore, it will be important in a future study to better characterize the changes that MHS causes to specific fat depots in mice since these produce an important proportion of circulating miRs [32].

To study RR and potentially myocardial recovery, we used a model where HFpEF was still mild, although significant. Pulmonary congestion, a marker of heart failure, was absent except for HFD females and AngII males ($p=0.051$). That said, from a clinical perspective, pulmonary congestion is treated with diuretics, and an intervention involving an aerobic exercise program will not be initiated in a patient with this condition untreated.

Aging remains an unmet criterion in this study. We still do not know if reverse remodelling is as effective in an older animal with age-related myocardial abnormalities. The answer is probably no, but that doesn't mean some degree of reverse remodelling couldn't be achieved. In HFpEF patients, the benefits of exercise are associated with a decrease in hospitalizations and an increase in quality of life [33–35]. Cardiac benefits are less evident, suggesting that the effects we observed in our young adult mice may be less in older animals. Another difference between humans and mice is that a sedentary lifestyle is not a choice for the latter. What we call voluntary training is more of a return to a normal lifestyle for these animals [36–38]. This also lowers the stress of life in captivity.

Clinically, valve replacement in patients with aortic stenosis is where reverse remodelling can be observed. The phenotype of aortic stenosis patients shares many features with HFpEF patients. In these patients, depending on the level of heart damage present before the procedure, only a tiny proportion will see their condition improve in one year, and for the most part, the damage will remain stable [39]. The reasons why some individuals see their clinical state improve or remain stable and others deteriorate with similar heart damage to begin with remain unclear [39].

We observed that myocardial and circulatory miRNome did not respond similarly to the four weeks granted for myocardial recovery. The circulatory miRNome seemed to return to normal, but not the LV one, suggesting that abnormal processes were still active in the myocardium. Two hypotheses can be offered here. The first is that the changes in the circulatory and myocardial miRNomes observed following MHS were mainly a reaction seeking to reduce the harmful effects of the stress and that despite the four weeks of recovery, myocardial repair or protection processes were still necessary. The second is that the remaining alterations in the LV miRNome point toward abnormalities that are now irreversible to the myocardium. Both hypotheses are probably true in proportions that are still difficult to establish. The data obtained from transcriptomic studies or, here, on microRNAs rarely succeed in pointing to a single cause for a phenotype. Our observations highlight the complexity of the phenomena and mechanisms involved and their interrelations.

 doi:10.20944/preprints202406.1909.v1

Nevertheless, some observations seem essential to emphasize. Despite a myocardial miRNome profile still essentially abnormal, the circulating one now seemed to have returned to normal, suggesting that the contribution of cardiac microRNAs to the circulating miRNome is probably low in mice. In addition, non-cardiac tissues appear after RR to release a normalized microRNA content into the circulation. This does not mean that other factors (proteins, other RNAs, peptides…) produced by these tissues have also returned to normal, and this will have to be investigated in the future.

When we separate the MHS into its entities, namely AngII, a vasoconstrictor and hypertensive factor with pro-hypertrophic effects on the heart but also at the kidney level and the HFD, obesogenic stress, probably inducing some insulin resistance and alterations on adipose and liver tissues, we find ourselves in front of highly similar circulating miRNomes. This does not mean that the different miRNomes of the tissues contributing significantly to the circulating one have a similar response to these stresses but that the circulatory resultant is mostly identical. This is surprising, considering the adipose tissue is a primary producer of circulating microRNAs. Stresses with opposite effects on the visceral fat, such as AngII and HFD, did not result in miRNome profiles with marked differences.

We identified more than 215 different miRs modulated by the various stresses and possibly involved in the following cardiac remodelling and myocardial recovery. These miRs have several possible gene targets, making the total number very high. On the other hand, not all circulating miRs directly influence cardiac physiology and not all target genes and the proteins they encode are expressed at significant levels in the myocardium. In addition, other molecules, such as long non-coding RNAs acting as sponges and counterbalancing miRs effects, have not been studied here but probably would help offer a more complete picture [40].

Some miRs or families of miRs stand out as modulated in several of our experimental groups. Although many of them have been described before as associated with cardiac physiology, a more direct demonstration of their targets in the heart remains to be shown.

High levels of miR in the post-MHS myocardium may reflect both their inhibitory action on the expression of a factor associated with normal physiology or a way to inhibit a harmful stress-induced factor. This is probably true for a miR whose levels were lowered.

One such example where levels of a miR can lead to such conclusions is let-7i. Both in the myocardium and in the circulation, let-7i levels are increased after MHS. Myocardial levels remain high after the recovery period. Yet, let-7i has been shown to have lower levels in the heart of mice receiving AngII for 3 or 7 days, and its administration can reduce the expression of several genes associated with fibrosis and protect the heart [41]. It can be speculated that over a more extended period of exposure to MHS, the myocardium induces the expression of protective miRs to attenuate the pro-fibrotic action of chronically administered AngII.

If let-7i has an anti-fibrotic action in the heart, as mentioned above, but also in the lungs or arteries, it is instead a pro-fibrotic action that seems to have this same miR in the kidney [42]. These observations suggest that processes involving the conventional TGFbeta signalling pathway would be modulated inversely by the same miR.

Moreover, in the let-7 family, five (let-7a to let-7e) saw their levels decrease by the MHS and the reverse was observed for let-7f, g and i. This family of miRs has a highly conserved sequence and shares many possible targets [43]. Therefore, it seems that the different members of this family may differ in their actions or intervene at various times during stress, as here for MHS.

Focusing on a miR or a family of these is probably reductive to understanding the stress-related action leading to heart failure, as in our mice. However, these miRs remain potential circulating biomarkers to follow the evolution of a condition or treatment over time. Unfortunately, the answers obtained from circulating miR changes can be falsely reassuring. This study shows significant molecular myocardial abnormalities remain despite seemingly complete reverse remodelling at the morphological and functional levels and normalized circulatory miR profile.

We intended to identify differentially modulated miRs between male and female mice after MHS and RR. In the end, there were few sex differences, and we studied all the animals together. However, the heart response to the high-fat diet differed between male and female mice, the latter being more

 doi:10.20944/preprints202406.1909.v1

sensitive to this stress. Although we did not measure plasma inflammatory markers in mice fed the HFD but not receiving AngII, we observed that several of these markers were increased by MHS only in females and not males, suggesting a more acute inflammatory response in female mice. The HFD could be the causing factor. Interleukins 17a and 17f were markedly increased only in MHS females. In conjunction with the observation that miRs related to the control of the JAK-STAT and the TH17 cell differentiation are modulated, this offers new research avenues to explore and explain this sex difference towards HFD in our HFpEF model. Male mice fed a high-fat diet for an extended period (12-16 weeks) have been shown to increase the production of IL-17 [44]. We observed this in females after only four weeks. For this parameter, the male response to HFD may be slower than that of females. In addition, at the myocardial level, the inflammatory molecule profile may differ. Still, this sex difference was unexpected and deserves further study.

5. Future Perspectives

This study highlights an aspect of interest: inter-organ communication in developing HFpEF and possibly its treatment. Plasma microRNAs are only a part of the messages sent and received in these exchanges. Two recent publications have shown that inactivation of visceral white adipose tissue in mice or activation of brown adipose tissue can reverse the pro-hypertrophic action of AngII on the heart. In the case of epididymal white adipose tissue, its removal, blocking the formation of exosomes or administering miR-23a-3p, could stop the pro-hypertrophic action of AngII. In our study, miR-23a-3p was not modulated by MHS and was downregulated by AngII alone after 28 days [45].

For the brown adipose tissue, blocking its action through 3-adrenergic receptor knock-out (ADRB3KO) worsened cardiac myocardial hypertrophy and fibrosis induced by AngII, while its activation had a protective effect. The adverse impact of ADRB3KO was mediated by the presence of iNOS in exosomes produced by brown adipose tissue [46].

6. Study Limitations

This study used a two-hit model to induce HFpEF that resembles human HFpEF (Aidara). Although we were able to design and develop a model that includes hypertension and metabolic stress and studied it in both sexes, the model is still not representative of the entire spectrum of HFpEF patients. The number of comorbidities in patients is usually more significant. HFpEF patients are most of the time old, postmenopausal (women) and often suffer from atrial fibrillation, risk factors that we did not or could not include.

We did not monitor our mice's running activity. The animals were housed in groups of 3-5; thus, it would not have been possible. Since all trained mice showed better exercise capacity than untrained ones, we assume that VE was accompanied by increased physical activity. Also, it is well-known that females run more kilometres per day than males [47], but this did not result in better resistance to an exhaustion test.

It is probable that investigating the miRNomes after four weeks or waiting four weeks after their cessation may have led us to miss the early changes of different miRs that dissipated with time.

We chose not to concentrate on a microRNA over another by treating mice with exogenous miRs or blocking their action. We were more interested in changes in their profile with the evolution of HFpEF or reverse remodelling. By doing so, we did not look for a possible mechanism of their action on the observed phenomenon. Our study emphasizes the need to keep this multi-organ view of HFpEF, a multifactorial syndrome.

7. Conclusion

In conclusion, we showed extensive LV reverse remodelling after MHS was stopped and voluntary exercise was introduced in a cardiometabolic HFpEF murine model. This microRNA sequencing study shows that RR is associated with normalizing the plasma miRNome but not the

myocardial one. We also observed that the miRNomes of males and females did not show sex-specific differences, but the circulating inflammatory markers profile did.

Grants: The work was supported by grants from the Canadian Institutes for Health Research PJT-1665850 (to J. Couet and M. Arsenault) and from the Fondation de l'Institut universitaire de cardiologie et de pneumologie de Québec.

Declaration: The protocol was approved by the Université Laval's animal protection committee and followed the recommendations of the Canadian Council on Laboratory Animal Care (#2020-603 and #2023-1250).

Conflicts of Interest: The authors have no competing interests.

References

1. Ponikowski P, Voors AA, Anker SD, Bueno H, Cleland JGF, Coats AJS, Falk V, González-Juanatey JR, Harjola VP, Jankowska EA, Jessup M, Linde C, Nihoyannopoulos P, Parissis JT, Pieske B, Riley JP, Rosano GMC, Ruilope LM, Ruschitzka F, Rutten FH, van der Meer P; ESC Scientific Document Group. 2016 ESC Guidelines for the diagnosis and treatment of acute and chronic heart failure: The Task Force for the diagnosis and treatment of acute and chronic heart failure of the European Society of Cardiology (ESC) Developed with the special contribution of the Heart Failure Association (HFA) of the ESC. *Eur Heart J*. 37:2129-2200. 2016, doi: 10.1093/eurheartj/ehw128.
2. Kitzman DW, Shah SJ. The HFpEF Obesity Phenotype: The Elephant in the Room. *J Am Coll Cardiol*. 68:200-203, 2016 doi: 10.1016/j.jacc.2016.05.019.
3. Shah SJ, Kitzman DW, Borlaug BA, van Heerebeek L, Zile MR, Kass DA, Paulus WJ. Phenotype-Specific Treatment of Heart Failure with Preserved Ejection Fraction: A Multiorgan Roadmap. *Circulation.* 134:73-90, 2016 doi: 10.1161/CIRCULATIONAHA.116.021884.
4. Ho JE, Enserro D, Brouwers FP, Kizer JR, Shah SJ, Psaty BM, Bartz TM, Santhanakrishnan R, Lee DS, Chan C, Liu K, Blaha MJ, Hillege HL, van der Harst P, van Gilst WH, Kop WJ, Gansevoort RT, Vasan RS, Gardin JM, Levy D, Gottdiener JS, de Boer RA, Larson MG. Predicting heart failure with preserved and reduced ejection fraction clinical perspective. *Circ Heart Fail* 9:e003116, 2016. doi: 10.1161/CIRCHEARTFAILURE.115.003116.
5. Shah SJ, Kitzman DW, Borlaug BA, van Heerebeek L, Zile MR, Kass DA, Paulus WJ. Phenotype-specific treatment of heart failure with preserved ejection fraction. *Circulation* 134:73–90, 2016. doi: 10.1161/CIRCULATIONAHA.116.021884.
6. Heidenreich PA, Bozkurt B, Aguilar D, Allen LA, Byun JJ, Colvin MM, Deswal A, Drazner MH, Dunlay SM, Evers LR, Fang JC, Fedson SE, Fonarow GC, Hayek SS, Hernandez AF, Khazanie P, Kittleson MM, Lee CS, Link MS, Milano CA, Nnacheta LC, Sandhu AT, Stevenson LW, Vardeny O, Vest AR, Yancy CW. 2022 AHA/ACC/HFSA Guideline for the Management of Heart Failure: Executive Summary: A Report of the American College of Cardiology/American Heart Association Joint Committee on Clinical Practice Guidelines. Circulation. 2022 May 3;145(18):e876-e894. doi: 10.1161/CIR.0000000000001062. Epub 2022 Apr 1.
7. Anker SD, Butler J, Filippatos G, Ferreira JP, Bocchi E, Böhm M, Brunner-La Rocca HP, Choi DJ, Chopra V, Chuquiure-Valenzuela E, Giannetti N, Gomez-Mesa JE, Janssens S, Januzzi JL, Gonzalez-Juanatey JR, Merkely B, Nicholls SJ, Perrone SV, Piña IL, Ponikowski P, Senni M, Sim D, Spinar J, Squire I, Taddei S, Tsutsui H, Verma S, Vinereanu D, Zhang J, Carson P, Lam CSP, Marx N, Zeller C, Sattar N, Jamal W, Schnaidt S, Schnee JM, Brueckmann M, Pocock SJ, Zannad F, Packer M; EMPEROR-Preserved Trial Investigators. Empagliflozin in Heart Failure with a Preserved Ejection Fraction. N Engl J Med. 2021 Oct 14;385(16):1451-1461. doi: 10.1056/NEJMoa2107038.
8. Sachdev V, Sharma K, Keteyian SJ, Alcain CF, Desvigne-Nickens P, Fleg JL, Florea VG, Franklin BA, Guglin M, Halle M, Leifer ES, Panjrath G, Tinsley EA, Wong RP, Kitzman DW; American Heart Association Heart Failure and Transplantation Committee of the Council on Clinical Cardiology; Council on Arteriosclerosis, Thrombosis and Vascular Biology; and American College of Cardiology. Supervised Exercise Training for Chronic Heart Failure With Preserved Ejection Fraction: A Scientific Statement From the American Heart Association and American College of Cardiology. Circulation. 147:e699-e715, 2023. doi: 10.1161/CIR.0000000000001122.
9. Rao RA, Bhardwaj A, Munagala M, Abraham S, Adig S, Shen A, Hamad E. Sex Differences in Circulating Biomarkers of Heart Failure. Curr Heart Fail Rep. 2024 Feb;21(1):11-21. doi: 10.1007/s11897-023-00634-w. Epub 2023 Dec 7.
10. Jalink EA, Schonk AW, Boon RA, Juni RP. Non-coding RNAs in the pathophysiology of heart failure with preserved ejection fraction. Front Cardiovasc Med. 2024 Jan 8;10:1300375. doi: 10.3389/fcvm.2023.1300375.
11. Dzau VJ, Hodgkinson CP. RNA Therapeutics for the Cardiovascular System. Circulation. 2024 Feb 27;149(9):707-716. doi: 10.1161/CIRCULATIONAHA.123.067373. Epub 2024 Feb 26.

12. Sayed D, Hong C, Chen IY, Lypowy J, Abdellatif M. MicroRNAs play an essential role in the development of cardiac hypertrophy. Circ Res. 2007 Feb 16;100(3):416-24. doi: 10.1161/01.RES.0000257913.42552.23. Epub 2007 Jan 18. PMID: 17234972.
13. van Rooij E, Sutherland LB, Thatcher JE, DiMaio JM, Naseem RH, Marshall WS, Hill JA, Olson EN. Dysregulation of microRNAs after myocardial infarction reveals a role of miR-29 in cardiac fibrosis. Proc Natl Acad Sci U S A. 2008 Sep 2;105(35):13027-32. doi: 10.1073/pnas.0805038105. Epub 2008 Aug 22.
14. Bagnall RD, Tsoutsman T, Shephard RE, Ritchie W, Semsarian C. Global microRNA profiling of the mouse ventricles during development of severe hypertrophic cardiomyopathy and heart failure. PLoS One. 2012;7(9):e44744. doi: 10.1371/journal.pone.0044744. Epub 2012 Sep 14.
15. Marfella R, Di Filippo C, Potenza N, Sardu C, Rizzo MR, Siniscalchi M, Musacchio E, Barbieri M, Mauro C, Mosca N, Solimene F, Mottola MT, Russo A, Rossi F, Paolisso G, D'Amico M. Circulating microRNA changes in heart failure patients treated with cardiac resynchronization therapy: responders vs. non-responders. Eur J Heart Fail. 2013 Nov;15(11):1277-88. doi: 10.1093/eurjhf/hft088. Epub 2013 Jun 4.
16. Chen QY, Jiang YN, Guan X, Ren FF, Wu SJ, Chu MP, Wu LP, Lai TF, Li L. Aerobic Exercise Attenuates Pressure Overload-Induced Myocardial Remodeling and Myocardial Inflammation via Upregulating miR-574-3p in Mice. Circ Heart Fail. 2024 Feb 27:e010569. doi: 10.1161/CIRCHEARTFAILURE.123.010569. Epub ahead of print.
17. Rodrigues PG, Miranda-Silva D, Li X, Sousa-Mendes C, Martins-Ferreira R, Elbeck Z, Leite-Moreira AF, Knöll R, Falcão-Pires I. The Degree of Cardiac Remodelling before Overload Relief Triggers Different Transcriptome and miRome Signatures during Reverse Remodelling (RR)-Molecular Signature Differ with the Extent of RR. Int J Mol Sci. 2020 Dec 18;21(24):9687. doi: 10.3390/ijms21249687.
18. Iguchi T, Niino N, Tamai S, Sakurai K, Mori K. Comprehensive Analysis of Circulating microRNA Specific to the Liver, Heart, and Skeletal Muscle of Cynomolgus Monkeys. Int J Toxicol. 2017 May/Jun;36(3):220-228. doi: 10.1177/1091581817704975. Epub 2017 May 2.
19. Li H, Fan J, Yin Z, Wang F, Chen C, Wang DW. Identification of cardiac-related circulating microRNA profile in human chronic heart failure. Oncotarget. 2016 Jan 5;7(1):33-45. doi: 10.18632/oncotarget.6631.
20. Morishima M, Ono K. Serum microRNA-30d is a sensitive biomarker for angiotensin II-induced cardiovascular complications in rats. Heart Vessels. 2021 Oct;36(10):1597-1606. doi: 10.1007/s00380-021-01853-8. Epub 2021 Apr 16.
21. Huang D, Chen Z, Wang J, Chen Y, Liu D, Lin K. MicroRNA-221 is a potential biomarker of myocardial hypertrophy and fibrosis in hypertrophic obstructive cardiomyopathy. Biosci Rep. 2020 Jan 31;40(1):BSR20191234. doi: 10.1042/BSR20191234.
22. Withaar C, Lam CSP, Schiattarella GG, de Boer RA, Meems LMG. Heart failure with preserved ejection fraction in humans and mice: embracing clinical complexity in mouse models. *Eur Heart J*. 42:4420-4430, 2021. doi: 10.1093/eurheartj/ehab389.
23. Aidara ML, Walsh-Wilkinson E, Thibodeau SÈ, Labbé EA, Morin-Grandmont A, Gagnon G, Boudreau DK, Arsenault M, Bossé Y, Couet J. Cardiac reverse remodelling in a mouse model with many phenotypical features of heart failure with preserved ejection fraction: effects of modifying lifestyle. Am J Physiol Heart Circ Physiol. 2024 Feb 16. doi: 10.1152/ajpheart.00462.2023. Epub ahead of print.
24. Walsh-Wilkinson É, Aidara ML, Morin-Grandmont A, Thibodeau SÈ, Gagnon J, Genest M, Arsenault M, Couet J. Age and sex hormones modulate left ventricle regional response to angiotensin II in male and female mice. Am J Physiol Heart Circ Physiol. 2022 Oct 1;323(4):H643-H658. doi: 10.1152/ajpheart.00044.2022.
25. Walsh-Wilkinson E, Arsenault M, Couet J. Segmental analysis by speckle-tracking echocardiography of the left ventricle response to isoproterenol in male and female mice. *PeerJ*. 9:e11085, 2021. doi: 10.7717/peerj.11085.
26. Chang, L., Zhou, G., Soufan, O. and Xia, J. (2020) miRNet 2.0 - network-based visual analytics for miRNA functional analysis and systems biology. Nucl. Acids Res. (doi: 10.1093/nar/gkaa467).
27. Fan Y, Siklenka, K., Arora, SK., Ribeiro, P., Kimmins, S. and Xia, J. (2016) miRNet - dissecting miRNA-target interactions and functional associations through network-based visual analysis. Nucl. Acids Res. 44 W135–141.
28. Shannon P, Markiel A, Ozier O, Baliga NS, Wang JT, Ramage D, Amin N, Schwikowski B, Ideker T. Cytoscape: a software environment for integrated models of biomolecular interaction networks. Genome Res. 2003 Nov;13(11):2498-504. doi: 10.1101/gr.1239303.
29. Chang, L. and Xia, J. (2022) MicroRNA Regulatory Network Analysis Using miRNet 2.0 Transcription Factor Regulatory Networks, 185-204. Humana Press, New York, NY.
30. Fan Y. and Xia, J. (2018) miRNet: functional analysis and visual exploration of miRNA-target interactions in a network context Computational Cell Biology. Humana Press, New York, NY
31. Cai Z, Fang L, Jiang Y, Liang M, Wang J, Shen Y, Wang Z, Liang F, Huo H, Pan C, Shen L, He B. Angiotensin II Promotes White Adipose Tissue Browning and Lipolysis in Mice. Oxid Med Cell Longev. 2022:6022601, 2022. doi: 10.1155/2022/6022601.

32. Funcke JB, Scherer PE. Beyond adiponectin and leptin: adipose tissue-derived mediators of inter-organ communication. J Lipid Res. 2019 Oct;60(10):1648-1684. doi: 10.1194/jlr.R094060. Epub 2019 Jun 17.
33. Crisci G, De Luca M, D'Assante R, Ranieri B, D'Agostino A, Valente V, Giardino F, Capone V, Chianese S, Rega S, Cocchia R, Israr MZ, Debiek R, Heaney LM, Salzano A. Effects of Exercise on Heart Failure with Preserved Ejection Fraction: An Updated Review of Literature. J Cardiovasc Dev Dis. 9:241, 2022. doi: 10.3390/jcdd9080241.
34. Fukuta H, Goto T, Wakami K, Kamiya T, Ohte N. Effects of exercise training on cardiac function, exercise capacity, and quality of life in heart failure with preserved ejection fraction: a meta-analysis of randomized controlled trials. Heart Fail Rev. 24:535-547, 2019. doi: 10.1007/s10741-019-09774-5.
35. Kitzman DW, Brubaker P, Morgan T, Haykowsky M, Hundley G, Kraus WE, Eggebeen J, Nicklas BJ. Effect of Caloric Restriction or Aerobic Exercise Training on Peak Oxygen Consumption and Quality of Life in Obese Older Patients With Heart Failure With Preserved Ejection Fraction: A Randomized Clinical Trial. JAMA. 315:36-46, 2016. doi: 10.1001/jama.2015.17346.
36. Casanova-Vallve N, Duglan D, Vaughan ME, Pariollaud M, Handzlik MK, Fan W, Yu RT, Liddle C, Downes M, Delezie J, Mello R, Chan AB, Westermark PO, Metallo CM, Evans RM, Lamia KA. Daily running enhances molecular and physiological circadian rhythms in skeletal muscle. Mol Metab. 61:101504, 2022. doi: 10.1016/j.molmet.2022.101504.
37. Maier G, Delezie J, Westermark PO, Santos G, Ritz D, Handschin C. Transcriptomic, proteomic and phosphoproteomic underpinnings of daily exercise performance and zeitgeber activity of training in mouse muscle. J Physiol. 600(4):769-796. doi: 10.1113/JP281535.
38. Kimura M, Suzuki S, Moriya A, Nogami K, Uchida R, Saito Y, Saito H. The Effects of Continuous and Withdrawal Voluntary Wheel Running Exercise on the Expression of Senescence-Related Genes in the Visceral Adipose Tissue of Young Mice. Int J Mol Sci. 22:264, 2020. doi: 10.3390/ijms22010264.
39. Généreux P, Pibarot P, Redfors B, Bax JJ, Zhao Y, Makkar RR, Kapadia S, Thourani VH, Mack MJ, Nazif TM, Lindman BR, Babaliaros V, Vincent F, Russo M, McCabe JM, Gillam LD, Alu MC, Hahn RT, Webb JG, Leon MB, Cohen DJ. Evolution and Prognostic Impact of Cardiac Damage After Aortic Valve Replacement. J Am Coll Cardiol. 2022 Aug 23;80(8):783-800. doi: 10.1016/j.jacc.2022.05.006. Epub 2022 May 17.
40. Uchida S, Dimmeler S. Long noncoding RNAs in cardiovascular diseases. Circ Res. 2015 Feb 13;116(4):737-50. doi: 10.1161/CIRCRESAHA.116.302521.
41. Wang X, Wang HX, Li YL, Zhang CC, Zhou CY, Wang L, Xia YL, Du J, Li HH. MicroRNA Let-7i negatively regulates cardiac inflammation and fibrosis. Hypertension. 2015 Oct;66(4):776-85. doi: 10.1161/HYPERTENSIONAHA.115.05548. Epub 2015 Aug 10.
42. Peng Z, Guo HY, Li YQ, Li JC, Yang XH, Liu J, Hu QD, Wang HL, Wang L. The Smad3-dependent microRNA let-7i-5p promoted renal fibrosis in mice with unilateral ureteral obstruction. Front Physiol. 2022 Aug 25;13:937878. doi: 10.3389/fphys.2022.937878.
43. Roush S, Slack FJ. The let-7 family of microRNAs. Trends Cell Biol. 2008 Oct;18(10):505-16. doi: 10.1016/j.tcb.2008.07.007. Epub 2008 Sep 4.
44. Surendar J, Frohberger SJ, Karunakaran I, Schmitt V, Stamminger W, Neumann AL, Wilhelm C, Hoerauf A, Hübner MP. Adiponectin Limits IFN-γ and IL-17 Producing CD4 T Cells in Obesity by Restraining Cell Intrinsic Glycolysis. Front Immunol. 2019 Oct 29;10:2555. doi: 10.3389/fimmu.2019.02555.
45. Su M, Li W, Yuan Y, Liu S, Liang C, Liu HE, Zhang R, Liu Y, Sun LI, Wei Y, Li C, Han X, Hao H, Zhao X, Luo Y, Yan S, Pan Z, Li Y. Epididymal white adipose tissue promotes angiotensin II-induced cardiac fibrosis in an exosome-dependent manner. Transl Res. 2022 Oct;248:51-67. doi: 10.1016/j.trsl.2022.05.004.
46. Lin JR, Ding LL, Xu L, Huang J, Zhang ZB, Chen XH, Cheng YW, Ruan CC, Gao PJ. Brown Adipocyte ADRB3 Mediates Cardioprotection via Suppressing Exosomal iNOS. Circ Res. 2022 Jul 8;131(2):133-147. doi: 10.1161/CIRCRESAHA.121.320470.
47. Novak CM, Burghardt PR, Levine JA. The use of a running wheel to measure activity in rodents: relationship to energy balance, general activity, and reward. Neurosci Biobehav Rev. 2012 Mar;36(3):1001-1014. doi: 10.1016/j.neubiorev.2011.12.012. Epub 2012 Jan 2.